International Journal of Pharmaceutics, 62 (1990) 165–186
Elsevier

IJP 02098

The collapse temperature in freeze drying: Dependence on measurement methodology and rate of water removal from the glassy phase

Michael J. Pikal and Saroj Shah

Lilly Research Laboratories, Eli Lilly & Co., Indianapolis, IN 46285 (U.S.A)

(Received 10 August 1989)
(Modified version received 11 December 1989)
(Accepted 17 January 1990)

Key words: Freeze drying; Lyophilization; Collapse temperature; Water mobility; Glass transition

Summary

Accurate determination of the maximum allowable product temperature during primary drying is critical to optimization of the freeze drying process. For an amorphous solute system, this maximum temperature is normally the collapse temperature. Methodologies for determining the collapse temperature involve direct microscopic observation of collapse during freeze drying and methods which, in effect, determine the glass transition temperature of the amorphous phase. While one might be tempted to assume that the collapse temperature is a property only of the material, and independent of details of the measurement method, both theoretical concepts and limited experimental observations suggest that this assumption may not be wholly correct. The main objective of this research is to determine the magnitude of variations in measured collapse temperature caused by variations in experimental methodology. The approach taken is both experimental, using moxalactam di-sodium formulated with 12% mannitol as a model, and theoretical. The theoretical analysis is based on two fundamental concepts. Firstly, for collapse to be observed, viscous flow of the amorphous phase must occur over a finite distance during the measurement time. Secondly, during a freeze drying process, water is removed from the amorphous phase once the ice-vapor boundary recedes past the region of interest. Since water removal increases viscosity, viscous flow, and therefore, collapse is partially arrested, and the effective collapse temperature will be increased, the effect being greater the faster the sublimation rate. A quantitative model based on these concepts is developed with key parameters being evaluated by experimental studies. The observed variation in collapse temperature of moxalactam di-sodium with sublimation rate is quantitatively predicted by the theory. The theory is used to investigate differences between collapse temperatures determined by laboratory procedures and the observation of collapse in production processes. The collapse temperature will increase as the sublimation rate increases (i.e., as the solute concentration decreases), and at constant sublimation rate, the collapse temperature may increase as the surface area of the solid increases. In general, product freeze drying in a vial will collapse at a slightly higher temperature than collapse measured by the microscopic method. However, the calculated variations in collapse temperatures are modest (1–3°C). Collapse temperature and glass transition temperature, T_g', are not identical, the latter being slightly lower when measured at low rates of temperature increase. A secondary but important experimental result is that, contrary to some opinion in the literature, water in a glassy system has sufficient mobility to be in approximate 'equilibrium' with the ice phase during the relatively slow temperature changes relevant to freeze drying operations.

Introduction

The primary drying, or ice sublimation, stage of the freeze drying process is frequently the most

Correspondence: M.J. Pikal, Lilly Research Laboratories, Eli Lilly & Co., Indianapolis, IN 46285, U.S.A.

time consuming portion of the process, and an optimized process must operate near the maximum allowable product temperature. For a solute system which does not crystallize but remains amorphous, this maximum temperature is generally the collapse temperature, T_c (MacKenzie, 1966; Pikal, 1985). During primary drying above T_c, one observes loss of structure in the dried region adjacent to the ice-vapor interface due to a glass transition in the amorphous product (Bellows and King, 1972). That is, as the temperature increases, the viscosity of the amorphous solute phase decreases until sufficient flow occurs to result in loss of the pore structure. Collapse will normally be cause for rejection of that vial due simply to lack of "elegance". High residual water and prolonged reconstitution times are also common consequences of collapse in a product. It also is possible that the increased molecular mobility resulting from the glass transition would cause in-process degradation of the product. Here, the product temperature needs to be maintained below the glass transition temperature of the amorphous solute in the ice matrix, denoted T_g' (Franks, 1986; Levine and Slade, 1988). In our experience, in-process decomposition arising from collapse or exceeding T_g' is rare, and for the balance of this analysis, T_c is assumed to be the maximum allowable product temperature for primary drying. Since a temperature increase of only 1°C results in at least a 13% reduction in primary drying time (Pikal, 1985), but product collapse must be avoided, accurate determination of the collapse temperature is critical to process optimization.

Collapse temperatures are normally estimated by one of three methods: (1) direct microscopic observation of collapse during freeze drying a thin film of frozen solution (Pikal, et al., 1983a); (2) thermal analysis methods which measure T_g' (Nail and Gatlin, 1985; Franks, 1986; Levine and Slade, 1988; Williams and Polli, 1988), and (3) by measuring the electrical resistance (or conductance) as a frozen sample is warmed (Nail and Gatlin, 1985). This method depends on the sharp increase in mobility of charged species as the system passes through T_g'. Obviously, both methods (2) and (3) above make the assumption, $T_c = T_g'$. One might be tempted to assume that the collapse temperature, like the eutectic temperature, is a property of the material, and therefore is independent of the solution concentration, and independent of the method of measurement. However, the eutectic temperature is a first order thermodynamic transition while glass transitions are second order transitions which may depend on sample history and measurement procedure. The distinction between T_c and T_g' is subtle but possibly important. Collapse, as defined here, is the result of a glass transition in the dried region formed during primary drying, while T_g' refers to a glass transition in the amorphous phase in contact with ice. The discussion of the collapse phenomena by Bellows and King (Bellows and King, 1972) makes it clear that collapse is a dynamic phenomenon involving viscous flow which could, in principle, mean that T_c depends on the method of measurement even beyond the recognized ambiguities in a second order transition.

Some experimental evidence supports this speculation. The collapse temperature for sucrose (Bellows and King, 1972) increases as the solution concentration decreases. Likewise, using the freeze drying microscope method, we find that a 2% solution of povidone collapses about 2.5°C higher than a 10% solution. Primary drying is much faster in the 2% solution (1.4 mm/h at −30°C) than in the 10% solution (0.13 mm/h at −30°C), so the observed concentration effect may well be a drying rate effect. We also observe that a product based on lactose as an excipient, which shows a collapse temperature (microscopic method) of −30°C apparently freeze dries in vials at product temperatures up to about −28°C without showing signs of collapse.

The main objective of this research was to determine to what extent the collapse temperature depends on the details of the measurement process. The approach taken is partially experimental, using moxalactam di-sodium (a cephalosporin-like antibiotic) as a model, and partly theoretical. The theoretical treatment has, as its starting point, the concepts presented by Bellows and King (Bellows and King, 1972). The key point is that for collapse to be observed, viscous flow must occur over a finite distance during the measurement time

period. Our analysis is also based on the concept that during primary drying, removal of water from the amorphous phase occurs once the ice-vapor interface passes by the region of interest. Since water removal increases the viscosity, viscous flow and therefore, collapse, will be arrested, and the effective collapse temperature will be increased, the effect being greater the faster the primary drying rate. Because of these dynamic effects, $T_c > T_g'$, (provided the experimental temperature ramp rates are comparable for both T_c and T_g' measurements) although the difference may be negligible. Parametrizing the theory with thermodynamic and kinetic data for moisture desorption from formulated moxalactam di-sodium (100% amorphous), calculations are used to systematically investigate the quantitative effect of a number of measurement variables on the collapse temperature.

Experimental

Lactose and mannitol were USP while the cephalosporins were obtained from Eli Lilly & Co. The materials were then freeze dried below their collapse temperatures using procedures similar to those described elsewhere (Pikal, et al., 1990). All freeze dried materials were 100% amorphous (x-ray powder diffraction, microscopic examination under polarized light).

Collapse temperatures were measured by the freeze drying microscope technique (Pikal et al., 1983a). Dried product resistances, $\hat{R}_p$, were measured by the freeze drying microbalance method or the vial method, as indicated, using procedures described previously (Pikal et al., 1983a). Specific surface areas were measured by BET analysis of nitrogen adsorption (three point) using the 'Qantasorb' (Qantachrome Corp.).

Desorption isotherm measurements were made gravimetrically using a microbalance procedure (Pikal et al., 1983b, 1990). Here, a small sample on a microbalance at temperature T_1 is exposed to water vapor from a water or ice source at temperature T_2 until constant weight is reached. Thus, 'equilibrium' between the sample and the water source is defined in an operational sense by noting no further mass change with time ($< 0.01\%$/h).

Glass transition temperatures, T_g, were determined using a Perkin Elmer DSC-2 with sealed aluminum pans and heating rate of 20 °C/minute. The values of T_g were determined from the thermograms using the usual graphical procedure (Angell et al., 1967b). Samples of the desired water content were prepared by equilibrating freeze dried powder (residual water content by Karl Fischer titration) in desiccators containing saturated salt solutions. The increase in water content was evaluated gravimetrically with occasional checks by Karl Fischer titration. About 0.1% 'crystallinity', presumably mannitol, was observed (microscope) in high moisture samples containing mannitol. Reproducibility of T_g with independently prepared samples was within approx. ± 0.5 °C. Viscosity was determined for a concentrated solution of formulated moxalactam di-sodium in water (0.37 g water/ml) using a crude adaptation of the falling ball method (Van Wazer et al., 1963). In our case the falling ball was a no. 6 lead shot from a shot-gun shell. The solution was placed in a 10 ml graduated cylinder and the temperature adjusted by equilibrating in a water bath. The ball was gently placed on the solution and allowed to sink into the fluid. The time required for the ball to pass between two marks on the cylinder allowed calculation of the velocity of the falling ball, which in turn allows calculation of the viscosity (Van Wazer et al., 1963). Reproducibility was within a few percent.

The kinetics of water desorption from the amorphous moxalactam di-sodium phase were studied using essentially the same microbalance procedure described previously (Pikal et al., 1990). The only differences involve the sample preparation. In this research an amorphous slab of nominal surface area 0.53 cm^2 was prepared by uniformly covering the bottom of the 'secondary drying cell' (Pikal, et al., 1990) with finely ground freeze dried moxalactam di-sodium (freeze dried with 12% mannitol), removing all water by drying at high vacuum (10^{-6} mmHg) and 50 °C until constant sample weight was noted, and then allowing the sample to absorb water from an ice source until the desired water content was ob-

tained. The water sorption procedure was carried out at a sample temperature such that when the final water content was reached, the sample would be above the glass transition temperature. Thus, with time, the sample would flow over the bottom of the cell forming a circular slab of uniform thickness (≈ 0.2 mm) and smooth surface. The temperature was then lowered to the desired temperature for water desorption studies. Water desorption was carried out at pressures of $\approx 10^{-6}$ mmHg. Apparent changes in mass due to desorption of water from the cell and other balance components constitute background effects that were subtracted from the total observed rate of mass loss. Background effects normally dissipate quickly but they do limit how close to "time zero" one can collect reliable data. We were limited to about 180 s for experiments with samples prepared at moderate relative humidity (0.262 g water/ml) but limited to about 600 s for samples prepared at very high relative humidity (0.323 g water/ml). Experiments with samples prepared at the very high relative humidity were not particularly well behaved or reproducible. Unacceptable high background effects persisted for far longer in these experiments, presumably due to some condensation in the apparatus, than in the experiments which involved lower humidity during final equilibration. After the desorption experiment the sample was examined visually. Minimal shrinkage was observed and except for a few cracks on the surface, the sample surface remained smooth. Thus, there may have been a slight increase in effective surface area during the drying experiment.

Theoretical

Collapse, viscosity, and flow

Collapse in a given region results from surface tension induced viscous flow of the amorphous phase after the ice-vapor interface has moved past that region. In the schematic shown in Fig. 1, the structure of the freeze drying system is depicted as a channel, or pore, initially filled with ice and bounded by walls of the amorphous solute of thickness, $2l$. The ice position at time zero is noted at the top of the diagram. In this diagram, the ice

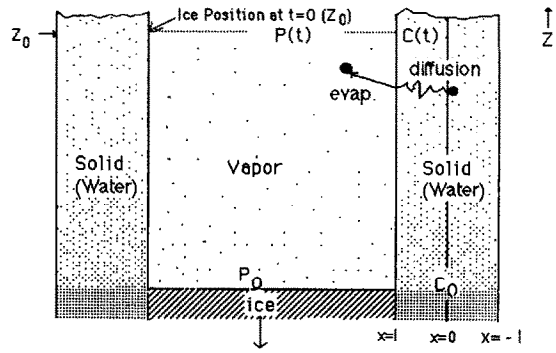

Fig. 1. A schematic of secondary drying during primary drying. At time zero, when the ice-vapor interface is at z_0, the partial pressure of water, in the pore adjacent to the solid is P_0 and the concentration of water in the solid pore wall is C_0. As sublimation proceeds and the ice-vapor interface moves down creating 'empty pore', the partial pressure of water vapor in the pore, $P(t)$, becomes less than P_0, and some drying of the solid occurs. Drying proceeds by diffusion from the interior of the solid with subsequent evaporation at the solid-vapor interface. The concentration of water in the solid at the interface, $C(t)$, becomes less than the initial concentration, C_0, and the glass transition temperature increases (i.e., the solid becomes more 'rigid').

has sublimed sufficiently to move down in the channel to a point near the bottom of the diagram. Here, the system freeze dried with retention of structure (i.e., the solid walls have not undergone viscous flow and therefore maintain their shape). If freeze drying had been conducted above the collapse temperature, the walls would have begun to flow once the ice-vapor interface had moved below the initial position, Z_0. If flow had persisted over a sufficient time to cause the pore walls to flow over a distance on the order of the pore radius, R, collapse would have been obvious.

We assume (Bellows and King, 1972) that surface tension, γ, is the 'driving force' causing flow, so the flow velocity, v, becomes: $v = 2\gamma/\mu$, where μ is the coefficient of viscosity. If collapse is observed over the observation time, TM, flow occurred over a distance on the order of R (the pore radius), and we may write

$$R = \int_0^{TM} v \, dt = 2\gamma \int_0^{TM} \frac{dt}{\mu(T,t)} \qquad (1)$$

where it is emphasized that the viscosity, μ, is a

function of both temperature, T, and time, t. While, in principle, surface tension may also depend on temperature and time, we make the plausible assumption that such dependencies are extremely small compared to corresponding dependencies in viscosity, and we assume the surface tension is a constant (an assumption consistent with our unpublished surface tension data on concentrated cephalosporin solutions above 0 ° C). The temperature dependence of the viscosity of a concentrated aqueous solution is non-Arrhenius at low temperature and may be written in the form (Angell, 1966, 1967a; Angell, et al., 1967a; Moynihan, 1966),

$$\mu(T,t) = A \exp\left(\frac{K}{T - k_2 T_g}\right) \tag{2}$$

where A, K and k_2 are constants and T_g is the glass transition temperature of the amorphous system as measured by DSC. The glass transition temperature depends only on the water content of the amorphous system. However, the water content is temperature dependent since the water content depends on the temperature dependent water activity. Here, we assume at least approximate equilibrium between water in the amorphous phase which is contact with ice and water in the ice, where water activity is given by the ratio of the vapor pressure of ice to the vapor pressure of pure supercooled liquid water at the same temperature. Note that our use of the term equillibrium refers only to transfer of water between phases on the time scale of the experiments described. The possibility that the amorphous phase itself is in a metastable state and perhaps subject to structural changes over a much longer time scale does not impact on this research. The water content in the amorphous solid (above the ice-vapor interface) is also time dependent due to secondary drying after the ice-vapor interface recedes. Therefore, the viscosity depends on both time and temperature.

Defining the collapse temperature, T_c, as that temperature which produces flow over distance 'R' in observation time 'TM', the collapse temperature is the solution of the equation,

$$\frac{2\gamma}{RA}\int_0^{TM} \exp\left(\frac{-K}{T_c - k_2 T_g}\right) dt - 1 = 0 \tag{3}$$

Eqn 3 is essentially the mathematical definition of collapse temperature and is developed by rearrangement of Eqn 1 with Eqn 2 used to substitute for viscosity.

Secondary drying during primary drying: Time dependence of surface water concentration

At time zero, the position of the ice-vapor interface is at Z_0, and the water in the amorphous solid is assumed to be in equilibrium with ice having vapor pressure 'P_0,' giving uniform water concentration, c_0, throughout the amorphous 'slab' of thickness $2l$ (Fig. 1). However, as the ice-vapor interface recedes, the fact that sublimation occurs demands that the partial pressure of ice at Z_0 be less than the partial pressure of ice at the ice-vapor interface, P_0. The partial pressure of water at Z_0 is time dependent, and is denoted, $P(t)$. Thus, as soon as the ice-vapor interface recedes from position Z_0, the amorphous phase, which contains a significant quantity of water, will begin to dry. Water will evaporate at the surface, and diffusion from the interior of the solid will transport water to the surface. The surface concentration of water, c_s, will then begin to decrease from its initial value, c_0, and the glass transition temperature of the amorphous phase at Z_0 will begin to increase in accordance with the water concentration dependence of T_g. To describe this phenomenon mathematically, we assume Fickian diffusion,

$$\frac{\partial c}{\partial t} = D\frac{\partial^2 c}{\partial x^2} \quad -l \leqslant x \leqslant l \tag{4}$$

with a surface evaporation boundary condition (Crank, 1956),

$$J = -D\left(\frac{\partial c}{\partial x}\right)_{x=\pm l} = \alpha[c_s - c_v(t)] \tag{5}$$

where D is the diffusion coefficient of water in the amorphous phase ($cm^2\ s^{-1}$), J is water flux ($g\ s^{-1}\ cm^{-3}$), c_s is the water content ($g\ cm^{-3}$) in the surface region (at Z_0 and $x = l$), and $c_v(t)$ is the (time dependent) concentration of water in the surface region that would be in equilibrium with the vapor in the pore at Z_0, $P(t)$, and α is the surface evaporation coefficient. The initial

boundary condition is $c(x,t=0)=c_0$. This model of course assumes, consistent with current concepts (Levine and Slade, 1988; Pikal et al., 1990), that the water is molecularly dispersed in the amorphous system forming a 'solid solution'.

The solution of Eqns 4 and 5 is outlined in Appendix I. The resulting expression for c_s as a function of time is used in conjunction with the experimental relationship for T_g as a function of water content to obtain the time dependence of T_g for use in Eqn 3. The collapse temperature, T_c, is then obtained by solution of Eqn 3 (see Appendix I for details). Input parameters required for the calculations are: (1) The dried product resistance parameter, $A1$, where $A1$ is defined in terms of the variation of the dried product resistance to vapor transport, $\hat{R}_p$, by: $\hat{R}_p = R_0 + A1 \cdot l$, where R_0 and $A1$ are constants, and l is the thickness of the dried product layer above the ice-vapor interface (Pikal, et al., 1983a); (2) the specific surface area of the freeze dried solid which is needed to estimate the thickness of the amorphous 'particles' (Appendix I); (3) The dependence of the glass transition temperature on water concentration; (4) the parameters for the viscosity equation (Eqn 2); the coefficient characterizing evaporation of water from the amorphous surface, α, and the diffusion coefficient, D; (5) the constant of proportionality between equilibrium water concentration in the amorphous phase and water activity (i.e., Henry's law is assumed), which is determined from water desorption isotherms; and (6) the sublimation rate parameter, $B1$, which is either evaluated from sublimation rate data or treated as an independent variable. $B1$ reflects the relative rate of decrease of partial pressure of water at position Z_0 (Fig. 1) and is proportional to the square of the temperature normalized sublimation rate (Appendix I).

Results and Discussion

Experimental data

Evaluation of input parameters for the theoretical calculations

Dried product resistance parameter, A1, and specific surface area The correlation between $A1$ values for moxalactam di-sodium systems and the solute concentration in wt% is shown in Fig. 2. At least as a first approximation, the resistance parameters are independent of method of resistance measurement (microbalance and vial methods) and independent of whether the formulation contains 12% mannitol or is pure moxalactam di-sodium. The data are, of course, specific to moxalactam di-sodium systems. The straight line in Fig. 2 is calculated data from the regression result, $A1 = 3.238\ (\text{wt\%})^{1/2}$. Note that here, and elsewhere in this section, the numerical parameters given (i.e., 3.238) are those used in the theoretical calculations, and the number of digits retained are not meant to suggest the level of 'experimental error'. These values of $A1$ refer to zero air pressure in the drying chamber. Adjustments for non-zero air pressure are made assuming that the 2% solid moxalactam di-sodium system (low resistance) shows the same relative air pressure effect as does 'low resistance' povidone and the 20 and 30%

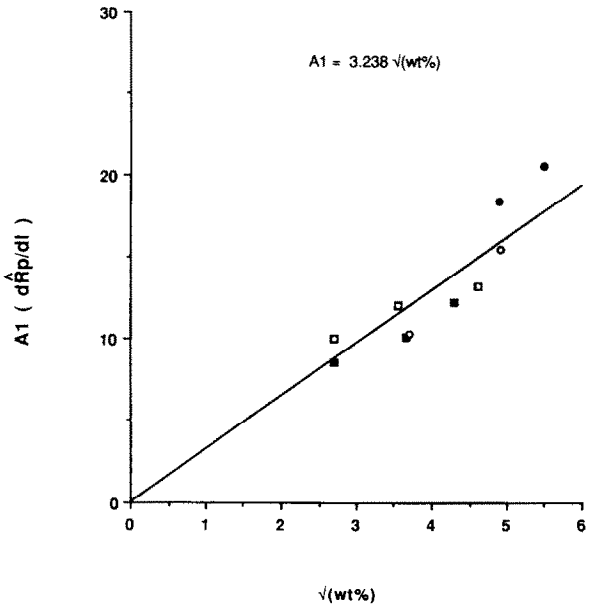

Fig. 2. The dried product resistance parameter, $A1$, for moxalactam di-sodium systems at $-25\,^{\circ}C$: dependence on concentration of solute in weight percent. Solid symbols refer to moxalactam di-sodium formulated with 12% mannitol, and the open symbols refer to pure moxalactam di-sodium. The squares refer to data generated with the microbalance method while the circles refer to measurements made on vial samples.

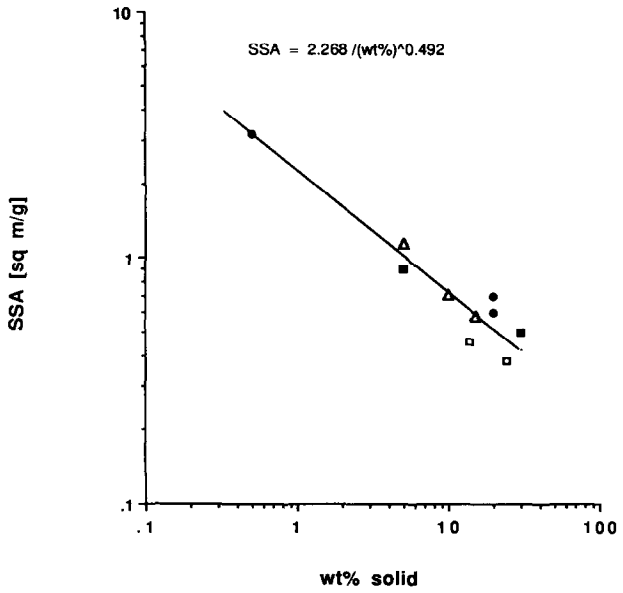

Fig. 3. Correlation of specific surface area (SSA) of some freeze dried amorphous solids with weight percent of solids in the original solution. Specific surface area is by BET analysis of nitrogen adsorption data. (■) moxalactam di-sodium with 12% mannitol; (□) pure moxalactam di-sodium; (△) lactose; (●) cephalothin sodium.

systems (high resistance) behave as does 'high resistance' KCl (Pikal et al., 1983a). The ratios, $Al(P)/Al$ ($P = 0$), for air pressures of 0.2 mmHg are 1.33 (povidone) and 1.04 (KCl), while for 1.0 mmHg the ratios are 2.67 (povidone) and 1.24 (KCl).

The correlation between BET specific surface areas in m^2g^{-1}, SSA, and solution concentration in wt% is shown in Fig. 3. At least for the solutes chosen, the correlation appears roughly independent of the chemical nature of the amorphous solid. The data for moxalactam di-sodium with 12% mannitol fall particularly close to the overall correlation line, $SSA = 2.268\ (wt\%)^{-0.492}$. While this correlation is strictly empirical, we note that since the total surface area of solute is determined by the surface area of ice crystals, one would expect that the surface area normalized for solute content, SSA, would decrease as the solute concentration increases as long as the ice crystal size is relatively insensitive to solute type and concentration.

Glass transition temperatures for moxalactam

Glass transition temperatures for moxalactam di-sodium systems are given in Fig. 4 as a function of water content of the amorphous phase in g/ml (note that all samples are > 99% amorphous). As expected, and similar to the corresponding data for povidone (MacKenzie and Rasmussen, 1972), increasing levels of water 'plasticize' the amorphous phase and decrease the glass transition temperature. The lines in Fig. 4 were calculated from empirical 'best fit' second degree polynomials. For moxalactam di-sodium formulated with 12% mannitol, the equation is:

$$T_g = 394.1 - 738.3c + 912.2c^2 \qquad (6)$$

The fit is within $\pm 0.5\,^{\circ}C$ in the concentration range of relevance to the collapse problem. Pure moxalactam di-sodium gives a similar relationship but with higher T_g values at corresponding water contents. Pure moxalactam di-sodium also has a higher collapse temperature measured by the microscopic method ($\approx 4\,^{\circ}C$ higher).

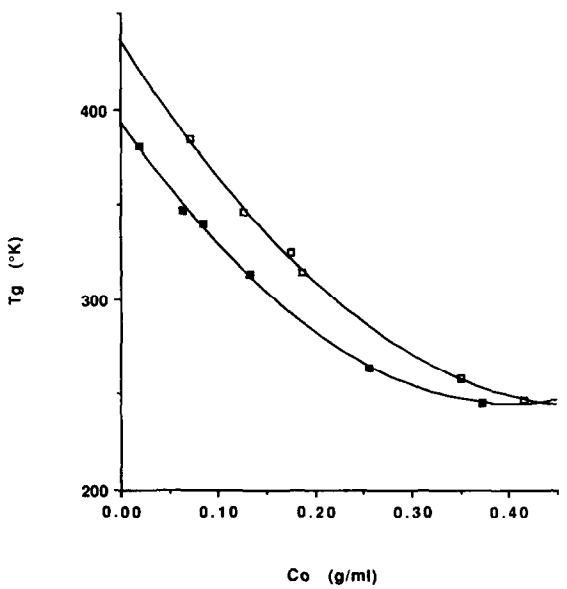

Fig. 4. Glass transition temperatures for moxalactam di-sodium systems as a function of water concentration. The water concentration in g/ml is estimated assuming additivity of volumes and a density of 1.5 g/ml for the anhydrous solid. (□) Pure moxalactam di-sodium; (■) moxalactam di-sodium formulated with 12% mannitol.

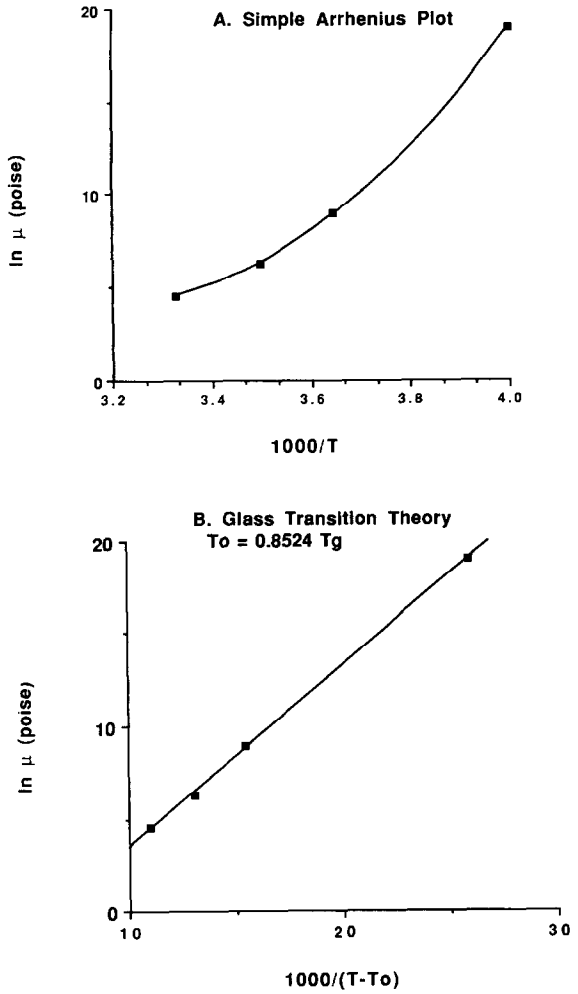

Fig. 5. Temperature dependence of the viscosity of aqueous moxalactam di-sodium formulated with 12% mannitol. The natural logarithm of the viscosity (μ) in poise is plotted.

Viscosity of moxalactam di-sodium / water systems: temperature dependence

The three data points at highest temperatures (Fig. 5) represent experimental measurements via the falling ball method on a solution of 0.37 g water/ml with $T_g = 245.81$ K (Eqn 6). The fourth 'data' point is calculated from the experimental collapse temperature with $B1 = 0$ of a 30% solids solution ($-23.1°$C) as follows: (1) At $-23.1°$C, the desorption isotherm data discussed in the next section (Fig. 6) give, $c_0 = 0.344$ g/ml. The use of Eqn 6 then gives $T_g = 248.07$ K ($-25.09°$C) for the glass transition temperature of the system undergoing collapse. (2) The value of the viscosity of the system undergoing collapse is calculated with Eqn 1 using $R = 5$ μm, and TM = 0.2 h, parameters appropriate for determination of the collapse temperature of a 30% moxalactam di-sodium solution by the freeze drying microscope method. Thus, during collapse, the viscosity is, $\mu = 1.814 \times 10^8$ P, and the fourth (T, T_{g_s} μ) data point is: (250.06 K, 248.07 K, 1.814×10^8 P).

With many viscous fluids, the temperature dependence is not Arrhenius in the sense that as the temperature approaches the glass transition temperature for the system, the viscosity increases much more rapidly than would be predicted by the Arrhenius expression. One equation capable of representing the observed temperature dependence is given by Eqn 2. Experimental viscosity data for formulated moxalactam di-sodium are plotted according the the Arrhenius expression in Fig. 5A and plotted according to Eqn 2 in Fig. 5B with the following best fit parameters: $K = 976$ K; $A =$

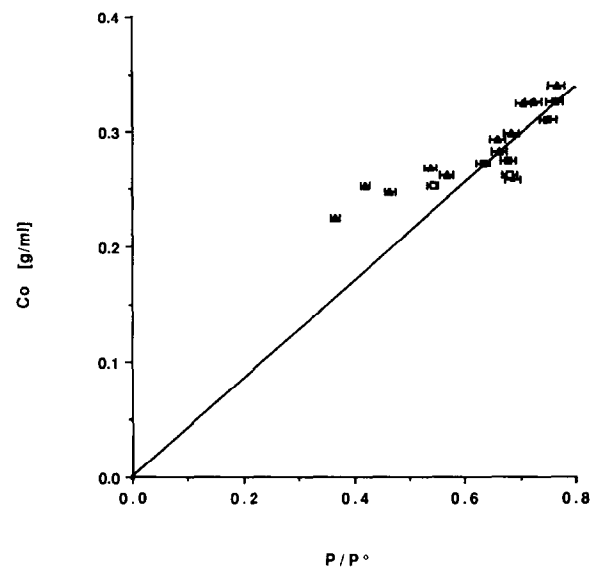

Fig. 6. Water desorption isotherms for moxalactam di-sodium formulated with 12% mannitol. The open symbols refer to a temperature of $-20.5°$C while the filled symbols refer to $-24.6°$C. The squares refer to samples in 'slab' geometry while the triangles refer to powder samples. The straight line defines the effective Henry's Law slope for the high relative pressure range.

1.90×10^{-3} P; and $k_2 = 0.8524 \pm 0.0309$. The Arrhenius plot is non-linear, even for the first three 'high temperature' experimental data points, but the plot according to the 'glass transition state' theory model (Eqn 2) is linear, as required. Of course, since the low temperature data point is based on a calculation which assumes the validity of Eqn 2, the comparison in Fig. 5 is not a sensitive test of the validity of Eqn 2. Rather, we assume the validity of Eqn 2 and note that the data are at least consistent with this assumption. The values for K and k_2 are reasonably close to the corresponding values typically found for simple ionic liquids: $K \approx 700$ K, $k_2 \approx 0.87$–0.95 (Angell, 1966, 1967a; Angell et al., 1967a; Moynihan, 1966).

Water desorption isotherms for moxalactam Water desorption isotherm data for moxalactam di-sodium formulated with 12% mannitol are given in Fig. 6. The data were generated by first exposing a dry sample to water from an ice source until mass transfer 'equilibrium' was reached, followed by a series of equilibrations with water vapor at decreasing partial pressure. With the powder samples, the last desorption step was followed with a water sorption step to check for hysteresis. No hysteresis was observed. The samples are in the glassy state at the temperature of the measurement below water concentrations of 0.34 g/ml ($-24.5\,^\circ$C) and 0.31 g/ml ($-20.5\,^\circ$C). Thus, with the exception of the powder samples at the start of the desorption experiment, all samples were glasses. The horizontal error bars represent the estimated uncertainty arising from estimated temperature measurement errors (i.e., resulting in errors in the relative pressure, P/P^*). No consistent trend with either sample form (i.e., slab or powder) or temperature is evident. The straight line, $c = 0.434$ (P/P^*), gives the best fit to the data above 0.28 g/ml consistent with the direct proportion demanded by Henry's law. The fact that this direct proportion only holds above 0.28 g/ml has little effect on the theoretical calculation of collapse temperature. Near the collapse temperature for moxalactam di-sodium, the water content is ≈ 0.34 g/ml, and a decrease in water content to 0.28 g/ml due to water removal from the amorphous phase results in an increase in T_g of about $10\,^\circ$C. This increase in T_g produces an increase in viscosity (Eqn 2) of more than three orders of magnitude, thereby arresting collapse, so the failure of Henry's law upon further drying and the resulting viscosity error is of no consequence.

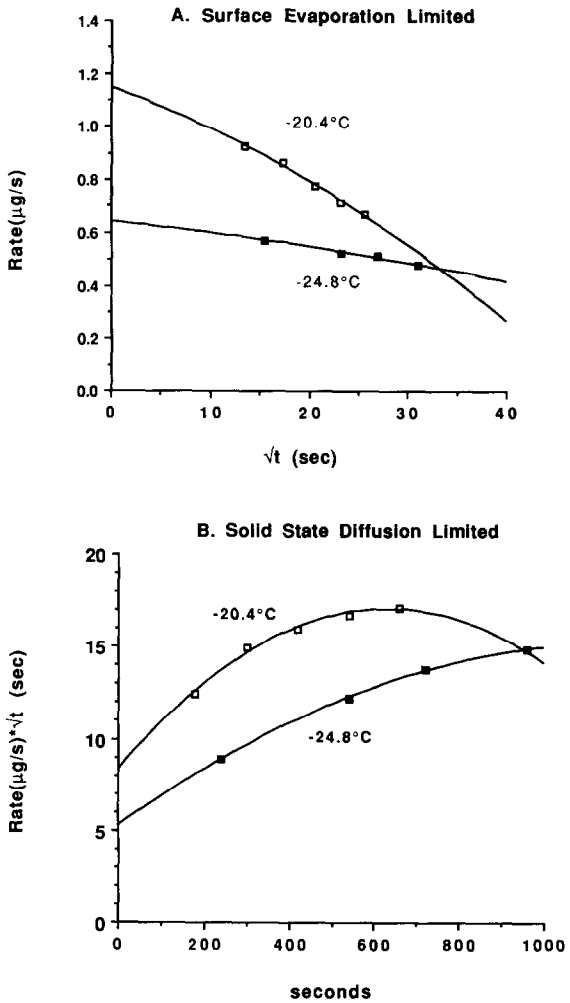

Fig. 7. Water evaporation kinetics for moxalactam di-sodium formulated with 12% mannitol. The initial water content is 0.262 g/ml, the slab surface area is 0.53 cm^2, and the thickness, l, is 0.018 cm. The open symbols refer to $-20.4\,^\circ$C while the filled symbols refer to $-24.8\,^\circ$C. The smooth lines represent quadratic fits to the data.

Kinetics of water desorption from glassy moxalactam: α and D evaluation Kinetic data for water removal from glassy formulated moxalactam di-sodium at high water content and low temperature are given in Fig. 7. These data form the experi-

mental basis for estimation of the surface evaporation parameter, α, and the diffusion coefficient, D. Theoretically (Appendix II), if the rate of water removal is controlled by surface evaporation with diffusion in the solid being at most a small perturbation, the rate should decrease linearly with the square root of time at small times (Fig. 7A). The evaporation coefficient, α, is evaluated from the time zero intercept while the limiting slope yields an estimate of the diffusion coefficient. Conversely, if diffusion in the solid is rate limiting for mass transfer, a plot of the product of rate and square root of time should be independent of time over the time course of the experiment (Fig. 7B), and this product determines the diffusion constant. The data are consistent with surface evaporation control (Fig. 7A), but since the 'rate $\cdot \sqrt{t}$' products are clearly time dependent, the data are not consistent with diffusion control. Therefore, we conclude that, at least for moxalactam di-sodium, mass transfer of water is surface evaporation controlled. As noted in Appendix II, the value of α depends on the water content. Adjusting the data from Fig 7A to a water content relevant to the collapse problem ($0.28 \leqslant c_0$ g/ml $\leqslant 0.35$) gives $\alpha = 4.4 \times 10^{-6} \pm 0.4 \times 10^{-6}$ cm/s at $-24.8\,^{\circ}$C. Because the limiting slope is quite uncertain, the most that can be concluded about the diffusion coefficient is that the magnitude is roughly 10^{-6}–10^{-7} cm^2/s.

The ability of water molecules to undergo translational motion in an amorphous system below the glass transition temperature, and therefore to 'equilibrate' with adjacent ice or to be removed during secondary drying on an experimental time scale, has been questioned in several recent reports (Franks, 1986; Levine and Slade, 1988). This point of view is based on extremely small diffusion coefficients estimated from application of the Stokes-Einstein equation and the concept that at equilibrium, all water would be in the form of ice. While use of the Stokes-Einstein equation to calculate the diffusion coefficient of water from the viscosity of the amorphous phase does predict essentially immobile water in glassy amorphous systems, the proper interpretation of this observation, in our opinion, is simply that the Stokes-Einstein equation is an inappropriate model for estimating translation motion of water in a glassy amorphous system. While the mobility of water certainly decreases dramatically as the system temperature decreases below the glass transition temperature, essentially zero mobility is not consistent with the data. Immobile water is clearly not consistent with the data in Fig. 7, regardless of whether the rate determining step is surface evaporation or diffusion in the solid. Furthermore, as detailed elsewhere (Pikal et al., 1990), secondary drying can be carried out at reasonable rates well below the glass transition temperature of amorphous water containing systems. Low but significant mobility of water in other glassy systems has also been reported (Garcia-Fierro and Aleman, 1985).

The concept that equilibrium implies all water is in the form of ice (or vapor) would be valid if water were the only component. That is, the free energy of water in ice is clearly lower than the free energy of liquid water at any temperature below $0\,^{\circ}$C. However, the system of interest to freeze drying also contains an amorphous solute. Interaction of water with the amorphous solid provides a mechanism to lower the free energy of the water which is molecularly dispersed in the amorphous solid. Equilibrium between water in ice and water in the amorphous phase is not only possible mechanistically, such equilibrium does occur in practice. The observation that water can be spontaneously transferred from an ice reservoir to an amorphous solid during a sorption or desorption isotherm experiment (Fig. 6; Pikal, et al, 1990) demonstrates that the free energy of water in the ice is initially higher than the free energy of water in the amorphous solid, and equilibrium is reached (no further mass transfer) only after the amorphous solid absorbs significant quantities of water. For example, the powder desorption isotherms shown in Fig. 6 were generated by first transferring water from an ice source at $\approx -20\,^{\circ}$C to the dried product at a slightly higher temperature. While mass transfer is slow (equilibration only after on the order of 10 h), spontaneous mass transfer does occur. Thus, an amorphous glass allowed to equilibrate with ice does contain a significant amount of 'dissolved' water, and such water is not necessarily kinetically 'trapped'.

Our arguments do assume that the thermodynamics and kinetics of moisture transfer from ice to amorphous solid via the vapor phase [H_2O (amorphous solid) → H_2O (vapor) → H_2O (ice)] is predictive of water transfer in the frozen solution. As discussed later, the glass transition temperature in frozen moxalactam di-sodium can be calculated accurately by a procedure which depends on the validity of this assumption. We therefore conclude that the rate of water removal or water absorption is fast enough so that approximate equilibrium between the amorphous phase and surrounding ice can be maintained if the rate of change of temperature with time is typical of the slow changes in freeze drying applications. The small impact of incomplete equilibrium on collapse temperature measurement will be addressed later. We emphasize that our use of equilibrium refers only to mass transfer on the time scale of the freeze drying process. Changes in the amorphous phase resulting from an approach to a global, or true thermodynamic, equilibrium over a much longer time scale may be relevant to the stability of the freeze dried product, but are irrelevant to the freeze drying process.

Collapse temperatures for moxalactam di-sodium

Collapse temperatures for aqueous moxalactam di-sodium formulated with 12% mannitol were measured as a function of drying rate and solution concentration (Table 1). Variation of drying rate for a given concentration was obtained by varying the pressure in the cold stage chamber via a controlled air leak. The drying rate was evaluated by timing the movement of the ice-vapor interface during primary drying at $-30\,^{\circ}C$. The collapse temperature on the same sample was then obtained by slowly increasing the sample temperature ($\approx 0.1\,^{\circ}C$/min near the expected collapse temperature) and noting the temperature at which collapse was first observed. The data entry for the 30% solution at 1 atm was obtained by first freeze drying under vacuum below the collapse temperature until a well defined dried region was established, venting to atmosphere, and then increasing the sample temperature slowly until collapse in the dried region was noted. The drying rates were reproducible to only about $\pm 20\%$ while collapse temperatures were generally reproducible within $\pm 0.5\,^{\circ}C$. The drying rate parameter, $B1$, was calculated from Eqn 8 using the experimental

TABLE 1

Experimental collapse temperatures for moxalactam di-sodium (with 12% mannitol)

Chamber pressure (mmHg)	Drying rate at $-30\,^{\circ}C$ (mm/h)	$B1$ ($mmHg^{-1}\,h^{-1}$)	Collapse temperature ($^{\circ}C$) [a]
2% (w/w) solute; $l = 0.414\ \mu m$ [b]			
0.0	1.86	1.76	−20.7
0.2	0.75	0.38	−22.0
1.0	0.51	0.35	−22.0
Mean	1.0	0.8	-21.6 ± 0.4
20% (w/w) solute; $l = 1.28\ \mu m$			
0.0	0.20	0.056	−21.4
0.2	0.32	0.149	−21.7
1.0	0.29	0.146	−22.7
Mean	0.27	0.12	-21.9 ± 0.04
30% (w/w) solute; $l = 1.57\ \mu m$			
0.0	0.51	0.40	−23.3
0.2	0.35	0.20	−23.6
1.0	0.16	0.049	−23.0
760.0 (1 atm)	0.00	0.000	−23.1
Mean	0.25	0.16	-23.2 ± 0.1

[a] Mean of at least two independent replicates. Replication is usually within $\pm 0.5\,^{\circ}C$.

[b] l (half-thickness of amorphous particle) is calculated from the specific surface area, which in turn is estimated from the correlation of specific surface area and concentration (Fig. 3).

drying rate, the vapor pressure of ice, P_0, at $-30\,^\circ$C, the volume fraction of ice, ϵ, and the dried product resistance parameter, $A1$, which is calculated from the correlation between solute concentration and $A1$.

With one exception, increased chamber pressure decreased the rate of drying, as expected. The zero pressure entry for the 20% solution shows an anomalous low drying rate. The mean drying rate, $B1$, and collapse temperature for all chamber pressures are given for each solution concentration. The mean of the 30% data, $-23.2\,^\circ$C, compares favorably with the value determined by Mackenzie (1983), $-24\,^\circ$C, particularly when it is realized that values from different laboratories and different raw material lots are being compared. There appears to be a slight decrease in collapse temperature for the 30% solutions relative to the more dilute solutions, and the fast drying 2% solution (zero chamber pressure) appears to have a higher collapse temperature than the slower drying systems ($P = 0.2$ and $P = 1.0$). However, these trends are only marginally outside the estimated experimental error, and the general question of variation in collapse temperature with concentration and drying rate is best addressed by the theoretical analysis given in the next section.

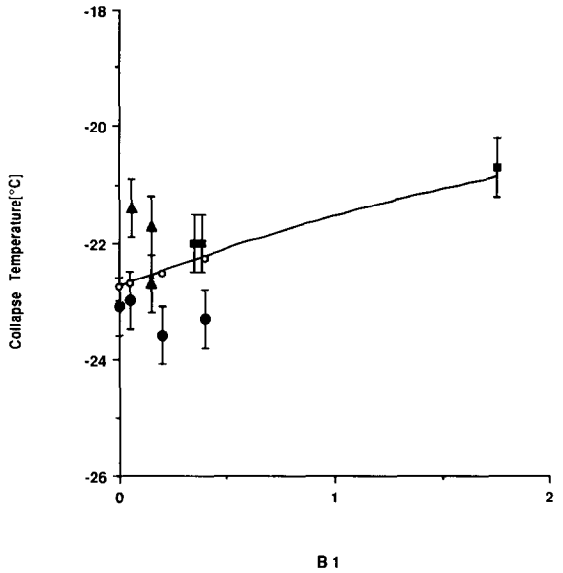

Fig. 8. Collapse temperatures for moxalactam di-sodium formulated with 12% mannitol as a function of the drying rate parameter, $B1$: A comparison of theory and experiment. A spatial resolution parameter, R, of 5 μm was used with a time of measurement, TM, of 0.2 h for the theoretical calculations. (———) Theory, for 2% solution; (○) theory, for 30% solution; (■) experimental, for 2% solution; (▲) experimental, for 20% solution; (●) experimental, for 30% solution.

Theoretical trends in collapse temperature

Comparison of theory and experiment

A comparison of theoretical and experimental collapse temperatures for formulated moxalactam di-sodium is illustrated by Fig. 8. Experimental collapse temperatures, sublimation rate parameters $B1$, and amorphous particle thickness parameters l were taken from Table 1. The theoretical collapse temperatures were calculated by fitting Eqn 3 to the collapse temperature data using the viscosity parameter, k_2, as an adjustable parameter. The resulting best fit value, $k_2 = 0.8542$, is used in generating all the theoretical data presented. The k_2 value obtained from the viscosity data alone, $k_2 = 0.8524$ (Fig. 5) differs only slightly, and the corresponding theoretical curves using $k_2 = 0.8524$ lie uniformly about 0.3 °C lower than the theoretical values shown in Fig. 8. Thus, the increase in collapse temperature over the range of experimental $B1$ values is 2.0 °C for either value of k_2. Note that since one of the viscosity data points was, in effect, calculated from the collapse temperature with $B1 = 0$, the close agreement between theory and experiment near $B1 = 0$ is a result of a 'forced fit'. However, it is significant that the observed increase in collapse temperature (2.0 °C) with increasing $B1$ is correctly predicted by the theory with no adjustable parameters. Note that the theoretical curves for 2% solution (solid line) and 30% solution (small open circles) are essentially identical, so at least according to the theory, the collapse temperature for formulated moxalactam di-sodium is essentially independent of solution concentration at constant $B1$. Experimentally, however, a change in concentration will normally change $B1$.

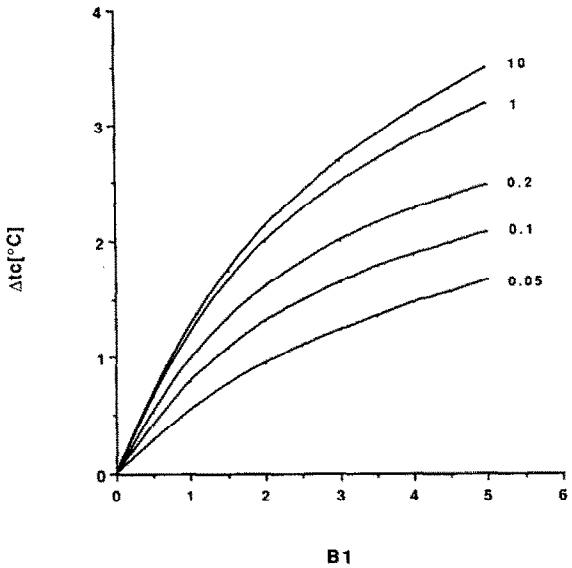

Fig. 9. The increase in collapse temperature with increasing drying rate parameter, $B1$, as a function of relative evaporation rate. The numbers next to each curve give the initial evaporation rate, α/l, relative to the initial evaporation rate for formulated moxalactam di-sodium with $l = 1$ μm. All other parameters are those for formulated moxalactam di-sodium. A spatial resolution parameter, R, of 5 μm was used with a time of measurement, TM, of 0.2 h.

Effects of sublimation rate and water evaporation rate

The effect of evaporation rate on collapse temperature (Fig. 9) is calculated to investigate the magnitude of collapse temperature changes for materials having different surface evaporation rates. The initial relative evaporation rate in vacuum, $-\mathrm{d}(m/m_0)/\mathrm{d}t$, where m_0 is the initial mass of water, is given (Eqn 5) by the ratio, α/l. This ratio is, in effect, an 'intrinsic' evaporation rate. Each curve represents the increase in collapse temperature of a hypothetical material as a function of the sublimation rate parameter, $B1$, for a given value of α/l. The number next to each curve is the corresponding value of α/l relative to the value of α/l for formulated moxalactam di-sodium with $l = 1$ μm. Thus, a large number means rapid evaporation (fast secondary drying), due either to a higher surface evaporation coefficient or a smaller particle thickness than a 1 μm moxalactam di-sodium particle. The temperature dependence of α and the Henry's law constant were assumed to be the same as for formulated moxalactam di-sodium.

As expected intuitively, a faster intrinsic evaporation rate results in a larger increase in collapse temperature at a given primary drying rate (i.e., fixed $B1$). However, even at high values of $B1$, the variation in collapse temperature is only about 2° C over a two order of magnitude range in intrinsic evaporation rates. That is, most materials should show modest variations in collapse temperature with variations in primary drying rate.

Effect of time of measurement, TM

The dynamic character of a collapse temperature measurement is illustrated by the time dependence of water concentration and viscosity in the surface region of the amorphous phase (Fig. 10). Calculations refer to formulated moxalactam di-sodium freeze drying in the freeze drying microscope with $B1$ and l values taken from Table 1. Both concentration (left axis) and viscosity (right axis) are normalized to their values at time zero, time zero being defined as the time when the ice-vapor interface moves past the region of interest. Since both the 'intrinsic' evaporation rate, α/l, and the sublimation rate parameter, $B1$, are higher for the 2% solution (Fig. 10A) than for the 30% solution (Fig. 10B), the rate of decrease of water concentration and the corresponding increase in viscosity are much greater for the 2% solution. After only about 0.1 h, the viscosity for the 2% solids system has increased by more than an order of magnitude. With such an increase in viscosity, flow will effectively cease, and collapse will be arrested. Thus, longer times of observation will not produce collapse, and the sample temperature must be increased above −23° to observe collapse. By contrast, the much smaller viscosity increase shown for the 30% system is not sufficient to arrest viscous flow, and collapse does occur at −23° C after observation periods of at least 0.2 h. Collapse at slightly lower temperatures will be observed if the observation time is longer.

While the collapse temperature for the 2% system (Fig. 10A) is not a function of the time of measurement, systems of lower sublimation rate parameter, $B1$, and/or lower "intrinsic" evapora-

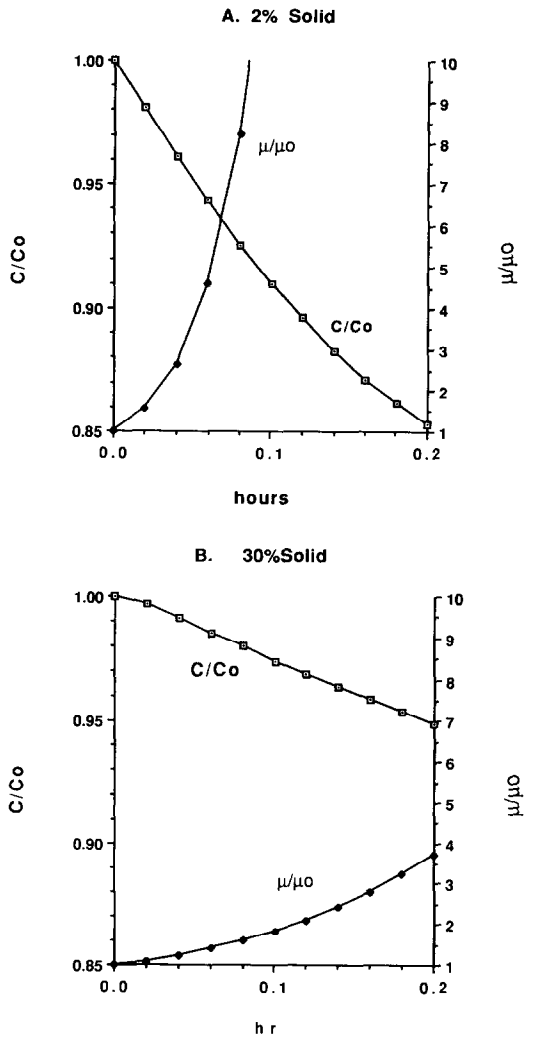

Fig. 10. Relative concentration and relative viscosity in solid formulated moxalactam di-sodium at $-23°C$ as a function of time after passage of the ice-vapor interface. The moxalactam di-sodium is assumed to be in equilibrium with ice at $-23°C$ prior to time zero (the ice-vapor interface passing the region of interest). Concentration, C, and viscosity, μ, are measured relative to their values prior to time zero, C_0, and μ_0, respectively.

tion rate, α/l, will show a dependence of collapse temperature on the time of measurement. The effect of variation in the time of measurement, TM, on collapse temperature is illustrated in Fig. 11. The calculations refer to systems having the same intrinsic evaporation rate as 2% formulated moxalactam di-sodium with the sublimation rate parameter treated as an independent variable. While the collapse temperature is essentially independent of the time of measurement above Bi values of 1.0, the time of measurement is a significant variable at very low Bi values. The time of measurement, TM, depends on the type of collapse observation, and in practice is somewhat ambiguous. For our microscope studies, we estimate TM ≈ 0.2 h, based on the time required to cause a significant change in temperature ($\approx 0.5°C$) during the continuous temperature ramp of $\approx 0.1°C$/min. However, observation of collapse during freeze drying in a vial at a fixed product temperature involves a time scale on the order of the primary drying time, which is at least several hours. The implication of Fig. 11 is that the collapse temperature measured by the microscopic method may be several degrees higher than found for production freeze drying if the system is characterized by a very low sublimation rate parameter. Such a low sublimation rate parameter, while perhaps rare, would be characteristic of a solute system that has a relatively high dried product resistance which is nearly independent of the

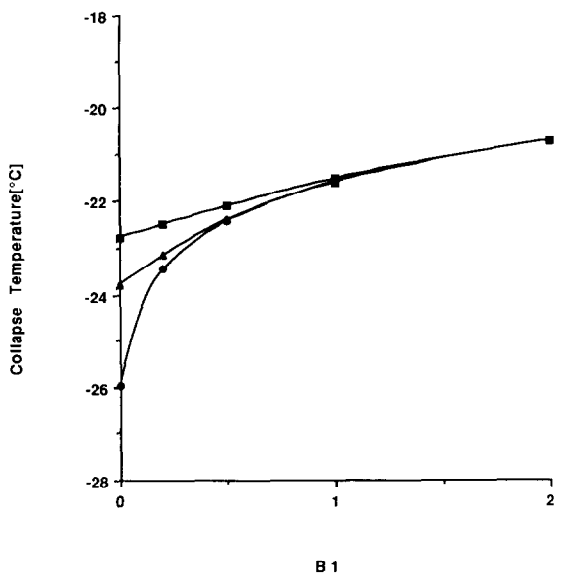

Fig. 11. The increase in collapse temperature with increasing drying rate parameter, Bi, as a function of time of measurement, TM. The parameters for formulated moxalactam di-sodium were used with $l = 0.414$ μm and a spatial resolution, R, of 5 μm. (■) TM = 0.2 h, (▲) TM = 0.5 h, (●) TM = 5 h.

thickness of the dried product, perhaps due to development of a relatively impermeable surface 'skin' (Pikal et al., 1983a).

Effect of variation in spatial resolution, R

Since viscous flow must occur over a finite distance before collapse is visually apparent, the spatial resolution inherent in the observation of collapse is a relevant variable for collapse determination either by the microscopic method or by visual inspection of a vial freeze dried product. As with the time of measurement parameter, the spatial resolution parameter is somewhat ambiguous. Our experience suggests that collapse is readily detected if flow occurs over a distance comparable to the pore radius in the freeze dried material, although other factors such as magnification in the microscopic method, color of the amorphous solid in visual inspection of a vial, and personal judgment also are involved to a lesser extent. Assuming that the pore radius is the best estimate of the spatial resolution parameter, a range of roughly 2–20 μm (measured via the light microscope or SEM) includes most materials we have studied. The value of 5 μm is typical of moxalactam di-sodium freeze drying in the freeze drying microscope and is the value of R used in all the previous calculations. The variation of collapse temperature with sublimation rate parameter for selected values of the spatial resolution parameter is shown in Fig. 12. The calculations were made using formulated moxalactam di-sodium parameters with the intrinsic evaporation rate equivalent to a 2% solution and TM = 0.2 h. A factor of two increase in spatial resolution parameter causes roughly a 1°C increase in collapse temperature. For a given material, differences in freezing rate can produce differences in pore size on the order of a factor of two (Pikal et al., 1983a), so differences in collapse temperature on the order of 1°C might be expected for systems subjected to major variations in freezing rate. Specifically, freezing in the freeze drying microscope is very fast relative to the freezing rate normally encountered in vial freeze drying. Consequently, the collapse temperature observed in production applications would be expected to be about 1°C higher than the collapse temperature

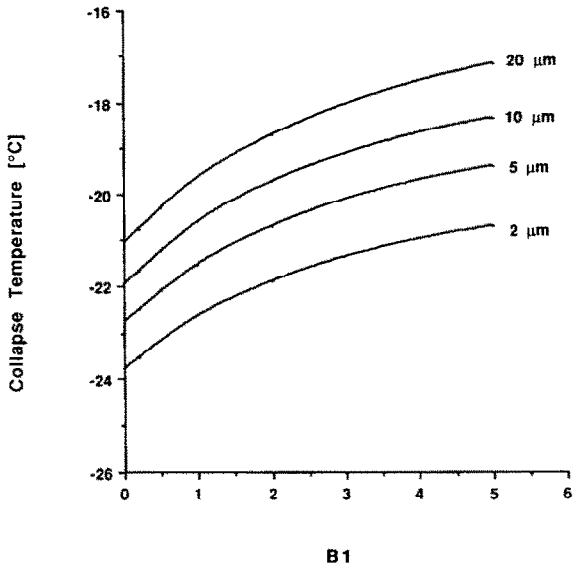

Fig. 12. The increase in collapse temperature with increasing drying rate parameter, $B1$, as a function of spatial resolution, R. Calculations were made using parameters for formulated moxalactam di-sodium with $l = 0.414$ μm and using a time of measurement, TM, of 0.2 h. The numbers next to the curves represent the corresponding values of R.

observed with the freeze drying microscope method—if all other parameters were held constant. However, in general, not all other parameters will be constant. An increase in pore size will also decrease the dried product resistance and therefore increase the value of $B1$, which will increase the collapse temperature. The longer TM for production freeze drying relative to microscopic observation will produce a lower collapse temperature for product freeze drying in a vial if the $B1$ value is small (Fig. 11), nearly canceling the increases caused by increased pore size. However, if sublimation is very rapid, as in a system of low solids content, the effect of variation in TM is negligible, and the net result expected is that the production sample will have a slightly higher collapse temperature (≈ 2°C) than the collapse temperature determined by the freeze drying microscope.

Comparison of collapse temperature with glass transition temperature

While both thermal analysis and electrical resistance analysis are used to estimate collapse tem-

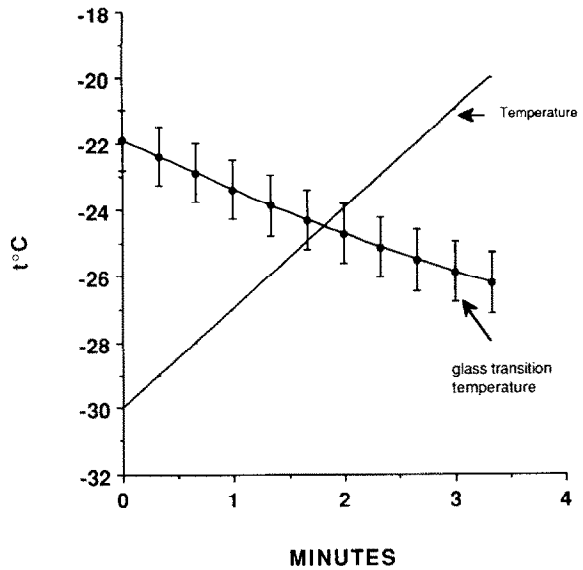

Fig. 13. The glass transition temperature for formulated moxalactam di-sodium in equilibrium with ice. The smooth line is the product temperature at a ramp speed of 3°C/min and the filled circles represent the calculated glass transition temperature of the amorphous phase.

perature, these methods measure the glass transition temperature of an amorphous phase in contact with ice. The glass transition temperature and the collapse temperature are not necessarily identical, although they are obviously closely related (Eqns 1 and 2). A graphical illustration of the 'mechanism' of a glass transition measured on a frozen system is given in Fig. 13 for formulated moxalactam di-sodium. As the product temperature of the frozen system is slowly increased, the water activity, P_0/P^* (Eqn 11), also increases. Assuming, for the moment, that the rate of temperature increase is slow enough so that equilibrium between ice and the amorphous phase is maintained, the water content of the amorphous phase increases in accordance with, $c = 0.434 \cdot (P_0/P^*)$. As the water content increases, the glass transition temperature of the amorphous phase, initially much higher than the product temperature, decreases (Eqn 6) and intersects with the product temperature curve (≈ 2 min in Fig. 13). At this point, the sample temperature is the glass transition temperature, T_g' (-24.5 ± 0.9°C), and the system undergoes a glass transition. The rather sizable estimated uncertainties are largely a result of temperature uncertainty in the water desorption isotherm studies. Note that the calculated glass transition temperature, -24.5 ± 0.9°C (Fig. 13), is only slightly lower than the collapse temperature measured at zero sublimation rate, -22.8 ± 0.3°C (Fig. 8), the difference of 1.7°C being only slightly outside the combined error estimates. However, since the collapse temperature increases as the rate of primary drying increases (Figs 8, 9), the glass transition temperature, T_g', could be significantly lower than the collapse temperature relevant for a system freeze drying at a high sublimation rate.

The glass transition temperature determination given by Fig. 13 assumes rapid equilibrium between ice and the amorphous phase in contact with ice. The fact that the result is in reasonable agreement with measurements on frozen formulated moxalactam di-sodium: −23.6°C (MacKenzie, 1983), −23.8°C (Williams and Polli, 1988), indicates the equilibrium assumption is at least a good approximation. However, equilibrium cannot be complete at a finite rate of sample temperature increase, and the water concentration in the amorphous phase must be slightly less than the equilibrium value, thereby increasing the measured glass transition temperature slightly. Assuming that the surface evaporation coefficient, α, found for evaporation into 'vacuum' is at least a useful approximation for water transport from ice to amorphous phase, one can estimate the magnitude of the effect from Eqn 5. In the context of the ice-amorphous phase equilibrium problem, the time dependent concentration, $c_v(t)$, in Eqn 5 represents the concentration of water in the solid which would be in equilibrium with the ice, and therefore, the difference, $c_s - c_v(t)$, is the deviation of the water concentration in the surface region from its equilibrium value. The flux, J, may be written: $-J = (dc/dt) \cdot (1/l)$, where l is the half-thickness of the amorphous phase. Taking the rate of concentration change as the rate required to maintain equilibrium for a given rate of temperature increase, the corresponding deviation from equilibrium required to maintain this water transport, $c_s - c_v(t)$, may be roughly estimated. At a typical rate of temperature increase of 3°/min

(MacKenzie, 1983; Williams and Polli, 1988), using $\alpha = 5 \times 10^{-6}$ cm/s and $l = 1$ μm, yields a relative deviation of water concentration from the equilibrium value of about 1%. With water concentration 1% lower than equilibrium, the glass transition temperature-time curve is about 0.3° C higher than the equilibrium curve shown in Fig. 13, giving $T_g' = -24.2$° C. For other materials, or with temperature increase rates significantly larger than 3° C/min, this non-equilibrium effect could be much larger than the +0.3° C estimated for formulated moxalactam di-sodium. Thus, the effect of temperature ramp rate on the measured glass transition temperature should be experimentally investigated when estimating collapse temperatures from DSC or electrical resistance data. Finally, we note that at the low temperature ramp rate used in the microscopic evaluation of collapse (≈ 0.1° C/min), this non-equilibrium effect is negligible.

Conclusions

The collapse temperature is not a unique property of the solute material being studied. The collapse temperature will increase as the sublimation rate increases (i.e., as the solute concentration decreases), and at constant sublimation rate, the collapse temperature may increase as the surface area of the solid increases. Differences in resolution and time of observation may cause small differences between the collapse temperature measured by the microscopic method and collapse observed in a product freeze drying in a vial. In general, the product freeze drying in a vial will collapse at a slightly higher temperature. However, the calculated (and observed) variations in collapse temperature noted above are modest (≈ 1–3° C). To minimize the variation between laboratory measurement of collapse temperature and production behavior, the collapse temperature measurements should be conducted using solute concentrations comparable to the concentrations of ultimate interest in production.

Collapse temperature and glass transition temperature, T_g', as measured by thermal analysis or electrical resistance analysis, are not identical. The glass transition temperature measured at very low temperature ramp rates will be slightly lower than the collapse temperature measured during sublimation drying. However, T_g' will increase slightly as the ramp rate increases.

The experimental observations on rate of removal of water from glassy moxalactam di-sodium, as well as our analysis of glass transition temperature measurements, indicate that the water in a glassy system has sufficient mobility to be in approximate equilibrium with the ice phase during the relatively slow temperature changes relevant to freeze drying operations. Further, water is capable of being removed at significant rates during secondary drying operations well below the glass transition temperature of the amorphous phase.

Appendix I: solution of the diffusion equation and details for the calculation of collapse temperature

To obtain a solution of the diffusion equation (Eqn 4) subject to the surface evaporation boundary condition (Eqn 5), we must first relate concentration of water in the amorphous solid, c, to partial pressure of water vapor, P. Here, we assume Henry's law, $P = k_H c$. At the surface, $x = l$, we have, $P_s = k_H c_s$, where P_s is the equilibrium vapor pressure of water arising from water concentration c_s, and $P(t) = k_H c_v(t)$. Substituting partial pressures for concentrations, the surface evaporation boundary condition may be expressed in a form more compatible with kinetic theory (Dushman and Lafferty, 1962), $J = (\alpha/k_H)[P_s - P(t)]$, where α/k_H would be a kinetic constant for evaporation, k_v.

Before the differential equation can be solved, we need to know c_v/c_0 so the surface evaporation boundary condition may be specified. First we note that, since we assume Henry's law, $c_v/c_0 = P(t)/P_0$. From the moving boundary model for ice sublimation presented by Mellor (1978), one may evaluate the change in partial pressure of water at a fixed position, Z_0, as a function of time expired after the ice-vapor boundary has receded

from Z_0. The result [1], valid to 2nd order in time t, is,

$$P(t) = P_0(1 - \beta t + 1.5\beta^2 t^2) \tag{7}$$

where,

$$\beta = Bl \cdot P_0; \quad Bl = \left(\frac{\rho_0 \cdot \epsilon \cdot Al}{P_0^2}\right)\left(\frac{dz}{dt}\right)^2 \tag{8}$$

The parameter, Al, is the dried product resistance parameter defined earlier. The derivative, dz/dt, is the rate of ice-vapor boundary movement at Z_0, which in the case of the chamber pressure being significantly less than the vapor pressure of ice, may be written in terms of the resistance of the dried product: $dz/dt = P_0/(\hat{R}_p \rho_0 \epsilon)$, where ρ_0 is the density of ice, and ϵ is the volume fraction of ice in the frozen product, and $\hat{R}_p$ is the dried product resistance at Z_0. Thus, substitution for dz/dt gives: $Bl = Al/(\hat{R}_p^2 \rho_0 \epsilon)$, with units of $(\text{mmHg})^{-1}\ \text{h}^{-1}$. Note that Bl is independent of time and temperature but does depend on the nature of the material being freeze dried.

The differential equation may be reduced to a form discussed by Carslaw and Yaeger (Carslaw and Yaeger, 1959) by substitution of a reduced concentration, y, for c, where, $y = (c_0 - c)/c_0$, giving

$$\frac{\partial y}{\partial t} = D\frac{\partial^2 y}{\partial x^2} - l \leqslant x \leqslant l$$

$$y(x, 0) = 0$$

$$\left(\frac{\partial y}{\partial x}\right)_{x = \pm l} = h[\Phi(t) - y] \tag{9}$$

where $h = \alpha/D$, and in our case, $\Phi(t) = \beta t - 1.5\beta^2 t^2$. This form of $\Phi(t)$ follows from the definition of reduced concentration, y, Henry's law, and the time dependence of water partial pressure given by Eqn 7. Eqn 9 is exactly the same in form as the analogous heat transfer equations considered by Carslaw and Yaeger, and the solution may be found by an application of Duhamel's theorem (Carslaw and Yaeger, 1959). Carslaw and Yaeger give a general solution for $y(x,t)$ where the function $\Phi(t)$ remains unspecified (their Eqn 1, p. 127). Going from Carslaw and Yaeger's general result to the expression we seek is laborious, but straightforward. The major steps in the derivation are: (1) perform the indicated (Carslaw and Yaeger, 1959) integration with $\Phi(t) = \beta t - 1.5\beta^2 t^2$; (2) obtain closed form expressions for the resulting infinite series terms not involving exponentials by using Fourier series; (3) evaluate $y(l,t)$ and drop terms of order L^2 and higher, where $L = \alpha\ l/D$. The resulting approximation is excellent as long as L is on the order of unity or less. The result may be written,

$$c_s = c_0\left\{1 - \beta t + 1.5\beta^2 t^2 - \frac{3\beta l^2}{\alpha} t + \frac{\beta l}{\alpha}\left[1 + \frac{3\beta l}{\alpha}\left(1 + \frac{L}{3}\right)\right] \cdot [1 - F(t)]\right\}$$

$$F(t) = \exp\left[\frac{-\alpha t}{l(1 + L/3)}\right] \tag{10}$$

Note that the assumption, $L < 1$, restricts the theory in its quantitative applications to water desorption kinetics which are surface evaporation limited with diffusion being a second order effect.

[1] The quadratic representation for $P(t)$ was necessary to obtain a tractable problem to solve for c_s. However, this function has a minimum at $\beta t = 1/3$, where $P/P_0 = 0.83$. Clearly $P(t)$ calculated from Eqn 7 ceases to have physical meaning at longer times where $\beta t > 1/3$. Due to the programing used, our numerical calculations require computer calculations for $\beta t > 1/3$. To avoid the computer increasing $P(t)$ at large t, we adopt the following calculation strategy. When $\beta t > 1/3$, at/l is very large, and c_s/c_0 is given simply by $P(t)/P_0$, which in closed form is, $(1 + 2\beta t)^{-1/2}$. Note also that when $\beta t > 1/3$, the value of c_s has decreased sufficiently such that T_g has increased significantly ($\approx 14°\text{C}$ for formulated moxalactam di-sodium), resulting in a very high viscosity and cessation of flow. Thus, when $\beta t > 1/3$ it makes little difference what we take as the exact value of c_s/c_0, and we use, $c_s/c_0 = (1 + 2\beta t)^{-1/2}$ for $\beta t > 1/3$.

In short, diffusion within the amorphous phase is fast compared to evaporation at the surface. This approximation seems most compatible with the data on water desorption kinetics (see Appendix II). However, it should be pointed out that even if diffusion in the amorphous phase were rate limiting, the theoretical results based on "diffusion limited" mass transfer would be qualitatively the same as we develop for the surface evaporation limited case. Further, since we do parametrize the theory using experimental mass transfer data, the quantitative predictions of the theory would also be similar.

The calculation of collapse temperature involves solving Eqn 3 for T_c. The calculations proceed as follows:

(1) The surface tension, γ, is taken as 63 dyne/cm. This value was estimated from an extrapolation of data on a concentrated (62% solid) cephalosporin solution, cefamandole nafate, extrapolated to $-23°C$. This value is close to the surface tension used for freeze dried foods (Bellows and King, 1972) of 70 dyne/cm.

(2) The value of the time of observation, TM, varies with the method of collapse observation. For freeze drying microscope procedures, TM is on the order of 0.2 h, while for collapse observed during freeze drying in a vial or in bulk, TM is on the order of hours. The value of the resolution parameter, R, is taken to be the average pore radius as determined by microscopic observation. For moxalactam di-sodium being freeze dried in a microscope apparatus, R is on the order of 5 μm.

(3) The viscosity parameters, A, K, and k_2 are evaluated from a fit of viscosity data for moxalactam di-sodium to the viscosity equation, Eqn 2 (with a final small adjustment in k_2 being made by a fit of collapse temperature data to Eqn 3).

(4) The glass transition temperature, T_g, for moxalactam di-sodium is experimentally determined as a function of water content in the amorphous phase, and the results expressed as a power series in water concentration (Eqn 6).

(5) The sublimation rate parameter, $B1$, is calculated from the dried resistance parameter, $A1$, and the rate of sublimation, dz/dt, using Eqn 8. $A1$ is determined from historical dried product resistance data, and dz/dt is either taken from directly measured rates (microscope data) at $-30°C$ and corrected to the temperature of interest, i.e., $dz/dt \propto P_0$, or alternately is calculated from historical dried product resistance data as described earlier.

(6) The half-thickness of the amorphous solid pore wall, denoted l is estimated from experimental specific surface area data using the pore model expression, $l = 1/\rho_s S'$, where ρ_s is the density of the amorphous solid (≈ 1.5 g/ml), and S' is the specific surface area of the freeze dried solid. Since S' is not available for samples studied by microscopy, S' is estimated from a correlation of specific surface area with concentration of solids in the aqueous solution being freeze dried.

(7) The concentration of water in the solid at time zero, c_0, is determined as a function of temperature from experimental water desorption isotherm data for formulated moxalactam di-sodium. Experimentally, $c_0 = k_A(P_0/P^*)$, where P_0 is the vapor pressure of ice at the temperature of interest (Pikal, 1985), and P^* is the vapor pressure of supercooled liquid water taken from a fit of CRC handbook data. The parameter, k_A, is independent of temperature over the small range of temperatures of interest. Vapor pressures are calculated from the expressions,

$$P_0(T) = 2.6983 \cdot 10^{10} \exp\left(-\frac{6144.96}{T}\right) \text{ (ice)}$$

$$P^*(T) = 6.362 \cdot 10^9 \left[\exp\left(\frac{-5750.38}{T}\right)\right] \cdot [1 - 0.0045(T - 273.16)] \text{ (liquid)} \tag{11}$$

(8) Experimental drying rates for formulated moxalactam di-sodium at high water content and low temperature were used to evaluate the surface evaporation parameter, α, and to estimate the diffusion coefficient. Diffusion coefficients are estimated to be large enough so that $L \approx 0$ is a good first approximation.

(9) The water concentration at the surface of the pore wall, c_s, is evaluated using Eqn 10 with the appropriate input parameters. Using this water

concentration, the glass transition temperature is calculated from the relationship between glass transition temperature and water concentration, and T_g is substituted in Eqn 3. Eqn 3 is then solved for the collapse temperature appropriate to the set of input parameters. All calculations were done using the numerical analysis program, MLAB (obtained from NIH).

Appendix II: details of surface evaporation coefficient and diffusion coefficient evaluations

The kinetic theory for evaporation rate from a surface (Dushman and Lafferty, 1962) suggests that surface evaporation flux, J, may be written in the form,

$$J = k_v(P_s - P_v) \tag{12}$$

where k_v is a kinetic constant for evaporation, P_s is the equilibrium vapor pressure of water in the amorphous phase at the solid-vapor boundary, and P_v is the partial pressure of water in the vapor space adjacent to the solid surface. In the experiments described by Fig. 7, $P_v = 0$. At water contents of 0.26 g/ml and lower, Henry's law is not obeyed (Fig. 6), but over a range in water content relevant to the collapse problem, linearity does exist, and we may write,

$$c_s = k_1 + k_A\left(\frac{P_s}{P^\cdot}\right) \tag{13}$$

where k_1 and k_A are constants independent of temperature over the small range of temperatures relevant to the collapse problem. Thus, Eqn 12 becomes,

$$J = \left(\frac{k_v}{k_A}P^\cdot\right)(c_s - k_1) \tag{14}$$

Eqn 14 is of the same form as the surface evaporation boundary condition given by Eqn 5 with, $\alpha = k_v P^\cdot/k_A$, and $k_1 = c_v$. However, in the context of Eqn 14, c_v $(= k_1)$ is independent of time. The data (Fig. 6) indicate that below an initial water content, c_0, of 0.27, $k_1 = 0.192$, and $k_A = 0.132$. Thus, for both temperatures (Fig. 7), $c_0 - k_1 = 0.0904$ g/ml.

Using the semi-infinite slab approximation [2] for Fickian diffusion with the surface evaporation boundary condition (Eqn 14), a closed form expression for the rate, $-\mathrm{d}m/\mathrm{d}t$, may be derived (Crank, 1956). However, numerical calculations and comparison of theory with experiment suggest that the model employed is valid only as a 'limiting law', valid for times close to time zero[2], so we expand the semi-infinite slab results in a power series in square root of time to obtain the limiting law expression,

$$-\frac{\mathrm{d}m}{\mathrm{d}t} = A_s\alpha(c_0 - k_1)\left(1 - \frac{2\alpha}{\sqrt{\pi D}}t^{1/2} + k_f t\right) \tag{15}$$

where D is the diffusion coefficient, α is the surface evaporation coefficient $(\alpha = k_v P^\cdot/k_A)$, t is time in seconds, and k_f is the coefficient of the linear term which, in principle, is a function of only α and D, but in practice also includes contributions from the failure of the semi-infinite model and other imperfections in the theory [2]. Values of α and D may be evaluated from the intercept and slope of the rate data plotted according to Eqn 15 (Fig. 7A). The values of α obtained are: $2.40 \times 10^{-5} \pm 0.19 \times 10^{-5}$ cm/s (-20.4°C) and $1.33 \times$

[2] Our numerical calculations comparing the semi-infinite slab with the finite slab (Crank, 1956) show that the semi-infinite slab (with evaporation from surface area A_s) is an excellent approximation to the finite slab (thickness, $2l$, with evaporation from area $2A_s$) up to evaporation of about 15% of the initial quantity of water. Note that a finite slab of thickness $2l$ with evaporation from both sides is equivalent to a finite slab of thickness l with evaporation from one side. The semi-infinite slab model fits the data over the entire time range of the experiments (Fig. 7), but the finite slab model is consistent with the data only up to about 400–500 s. At longer times, the finite model gives rates significantly lower than the experimental rates. This observation may be due to cracks in the slab increasing the surface area and/or shrinkage decreasing the effective thickness. Thus, the basic diffusion/evaporation model used is probably not quantitative except as a limiting law valid for times close to time zero.

$10^{-5} \pm 0.12 \times 10^{-5}$ cm/s ($-24.8°$C). Assuming Arrhenius temperature dependence,

$$\alpha = \alpha_0 \exp\left(-\frac{E_\alpha^*}{RT}\right) \tag{16}$$

with $\alpha_0 = 8.12 \times 10^{10}$ and $E_\alpha^* = 17.9$ kcal/mol. Because the limiting slope, which determines D, is rather uncertain, the most that can be concluded about the diffusion constant is: $D \approx 10^{-6} - 10^{-7}$ cm^2/s. It must be admitted that even 10^{-7} cm^2/s seems large given the magnitude of water diffusion coefficients in other glassy amorphous systems (Garcia-Fierro and Aleman, 1985).

Eqn 15 and therefore the values of α and D estimated above assume surface evaporation is rate limiting and diffusion has only a small effect on the kinetics. The opposite assumption states that diffusion is rate limiting and surface evaporation is very fast. With this assumption, the semi-infinite slab limiting law becomes,

$$\left(-\frac{dm}{dt}\right)\sqrt{t} = A_s c_0 \sqrt{\frac{D}{\pi}}\left[1 - 8F\left(\frac{Dt}{l^2}\right) + \ldots\right],$$

$$F(x) = \frac{\exp\left(-\frac{1}{x}\right)}{x} \tag{17}$$

The intercept of a plot of the product of rate and square root of time determines D (Fig. 7B). At $-20.4°$C, the calculated value of D is 1.1×10^{-8} cm^2/s. With this value of D, $F(Dt/l^2)$ is extremely small ($\approx 10^{-11}$) even near the end of the experiment, so the product of rate and square root of time should be constant. Experimentally, this product clearly is not constant (Fig. 7B). Alternately, the surface evaporation model predicts a finite drying rate at zero time with a negative limiting slope in a plot of rate vs square root of time, as observed (Fig. 7A). Because of these observations, we conclude that the surface evaporation model (Eqn 15) is more compatible with the data.

The values of α obtained from the data in Fig. 7A refer to a slab where c_0 is 0.262 g/ml, $k_1 = 0.192$ and $k_A = 0.132$. Yet, the collapse theory involves concentration in the range of 0.30 – 0.35 g/ml, where $k_1 = 0$, and $k_A = 0.434$. Since $\alpha = k_v P^*/k_A$, the value of α relevant to the collapse theory will obviously be different than the value determined from the data in Fig. 7A. Making the plausible, though somewhat arbitrary, assumption that the kinetic constant, k_v, is independent of water concentration over the range 0.26–0.35 g/ml, the value of α appropriate to the collapse application is given by adjusting the experimental value of α_0 (8.12×10^{10}) by the inverse ratio of k_A values, 0.132/0.434, thereby giving, $\alpha_0 = 2.47 \times 10^{10}$ ($0.28 \leqslant c_0 \leqslant 0.35$).

To provide a more direct measure of α for water concentrations in the range, $0.28 \leqslant c_0 \leqslant 0.35$, surface evaporation studies were attempted at $c_0 = 0.323$ and $t = -24.4°$C. However, due to erratic background effects, the measurements were not particularly reproducible at times near zero. Taking the average of four replicate runs and assuming the background fluctuations cancel, surface evaporation rates were obtained from 600 to 2100 s. The mean value for rate, $-dm/dt$, was 0.9 μg/s, with no obvious trend with time above the scatter in the data, ± 0.2 μg/s. The corresponding calculated value of α, assuming no time dependence, is $\alpha = 5 \times 10^{-6}$ cm/s, compared to the value calculated from Eqn 16 (with $\alpha_0 = 2.47 \times 10^{10}$) being, $\alpha = 4.6 \times 10^{-6}$ cm/s. The excellent agreement may be fortuitous, but at least provides support for the procedure used to calculate α for the collapse theory application from the data in Fig. 7A. With $\alpha \approx 5 \times 10^{-6}$ cm/s and $D \approx 10^{-7}$ cm^2/s, the value of L for a typical particle half-thickness in a freeze drying system is, $L \approx 5 \times 10^{-3}$. Thus diffusion of water in the solid is much faster than surface evaporation of water.

References

Angell, C.A., Free volume-entropy interpretation of the electrical conductance of aqueous electrolyte solutions in the concentration range 2–20 N. *J. Phys. Chem.*, 70, (1966) 3988–3998.

Angell, C.A., Viscous flow and electrical conductance in ionic liquids: Temperature and composition dependence in the light of the zero mobility concept. *J. Chem. Phys.*, 46 (1967a) 4673–4679.

Angell, C.A., Sare, E.J., and Bressel, R.D., Concentrated electrolyte solution transport theory: Directly measured glass

temperatures and vitreous ice. *J. Phys. Chem.,* 71 (1967b) 2759–2761.

Bellows, R.J. and King, C.J., Freeze-drying of aqueous solutions: maximum allowable operating temperature. *Cryobiology,* 9 (1972) 559–561.

Carslaw, H.S., and Jaeger, J.C., *Conduction of Heat in Solids,* 2nd Edn, Oxford Press, London, 1959.

Crank, J., *The Mathematics of Diffusion,* Oxford Press, London, 1956.

Dushman, S., and Lafferty, J.M., *Scientific Foundations of Vacuum Technique,* 2nd Edn, Wiley, New York, 1962.

Franks, F., Metastable water at subzero temperatures. *J. Microsc.* 141 (1986) 243–249.

Garcia-Fierro, J.L., and Aleman, J.V., Diffusion of water in glassy epoxide prepolymers. *Polym. Eng. Sci.,* 25 (1985) 289–294.

Levine, H., and Slade, L., Principles of cryostabilization technology from structure/property relationships of carbohydrate/water systems... A review. *Cryo-Letters,* 9 (1988) 21–63.

MacKenzie, A.P., and Rasmussen, D.H., Interactions in the water-polyvinylpyrrolidone system at low temperatures, in Jellinek, H.H.G., Ed. *Water Structure at the Water-Polymer Interface,* Plenum, New York, 1972, pp. 146–172.

MacKenzie, A.P. Basic principles of freeze-drying for pharmaceuticals. *Bull. Parenteral Drug Assoc.,* 20 (1966) 101–129.

MacKenzie, A.P., personal communication, 1983.

Mellor, J.D., *Fundamentals of Freeze Drying,* Academic Press, London, 1978.

Moynihan, C.T., The temperature dependence of transport properties of ionic liquids. The conductance and viscosity of calcium nitrate tetrahydrate and sodium thiosulfate pentahydrate. *J. Phys. Chem.,* 70 (1966) 3399–3403.

Nail, S.L., and Gatlin, L.A., Advances in control of production freeze dryers. *J. Parenteral Sci. Technol.,* 39 (1985) 16–27.

Pikal, M.J., Shah, S., Senior, D., and Lang, J.E., Physical chemistry of freeze-drying: measurement of sublimation rates for frozen aqueous solutions by a microbalance technique. *J. Pharm. Sci.,* 72 (1983a) 635–650.

Pikal, M.J., Lang, J.E. and Shah, S., Desolvation kinetics of cefamandole sodium methanolate: The effect of water vapor. *Int. J. Pharm..,* 17 (1983b) 237–262.

Pikal, M.J., Use of laboratory data in freeze drying process design: Heat and mass transfer coefficients and the computer simulation of freeze drying. *J. Parenteral Sci., Technol.,* 39 (1985) 115–138.

Pikal, M.J., Shah, S., Roy, M.L., and Putman, R., The secondary drying stage of freeze drying: drying kinetics as a function of temperature and chamber pressure, *Int. J. Pharm.,* 60 (1990) 203–217.

Van Wazer, J.R., Lyons, J.W., Kim, K.Y., and Colwell, R.E., *Viscosity and Flow Measurement,* Interscience, New York, 1963.

Williams, N.A., and Polli, G.P., Differential scanning calorimetric studies on frozen cephalosporin solutions. *Int. J. Pharm.,* 44 (1988) 205–212.